INSTRUMENTATION AND MEASUREMENT

Precision measurement and suppression of low-frequency noise in a current source with double-resonance alignment magnetometers

Jintao Zheng(郑锦韬)[1,2], Yang Zhang(张洋)[1,2], Zaiyang Yu(鱼在洋)[1,2,3], Zhiqiang Xiong(熊志强)[1,2], Hui Luo(罗晖)[1,2], and Zhiguo Wang(汪之国)[1,2,†]

[1] *College of Advanced Interdisciplinary Studies, National University of Defense Technology, Changsha* 410073, *China*
[2] *Hunan Key Laboratory of Mechanism and Technology of Quantum Information, National University of Defense Technology, Changsha* 410073, *China*
[3] *School of Physics and Information Technology, Shaanxi Normal University, Xi'an* 710049, *China*

(Received 5 July 2022; revised manuscript received 8 September 2022; accepted manuscript online 21 September 2022)

Low-noise high-stability current sources have essential applications such as neutron electric dipole moment measurement and high-stability magnetometers. Previous studies mainly focused on frequency noise above 0.1 Hz while less on the low-frequency noise/drift. We use double resonance alignment magnetometers (DRAMs) to measure and suppress the low-frequency noise of a homemade current source (CS) board. The CS board noise level is suppressed by about 10 times in the range of 0.001–0.1 Hz and is reduced to 100 nA/$\sqrt{\text{Hz}}$ at 0.001 Hz. The relative stability of CS board can reach 2.2×10^{-8}. In addition, the DRAM shows a better resolution and accuracy than a commercial 7.5-digit multimeter when measuring our homemade CS board. Further, by combining the DRAM with a double resonance orientation magnetometer, we may realize a low-noise CS in the 0.001–1000 Hz range.

Keywords: precision measurement, current noise suppression, low frequency, double-resonance alignment magnetometer

PACS: 06.20.fb, 06.30.Ka, 07.55.Jg **DOI:** 10.1088/1674-1056/ac9361

1. Introduction

Current source (CS) with low noise and high stability is of great significance for precision measurements, such as the calibration of units in metrology and the measurement of neutron electric dipole moment in fundamental physics.[1–6] In Refs. [1–6], one of the essential points to achieve high accuracy is the stability of CS. Therefore, some compensation methods should be used to suppress the current noise. Commonly, CS noise is suppressed by a feedback control system, which converts current into voltage with a high-precision resistor.[7] However, due to noise in electronic devices (for example, $1/f$ noise, thermal noise, and shot noise), it is challenging to effectively suppress low-frequency noise. A more accurate current measurement method in low frequency is needed to solve this problem. Fortunately, according to Ampere's law, current can be converted by a coil to a magnetic field, which can be measured by a magnetometer. At present, sensitivity of optically pumped magnetometers (OPMs) has reached the order of 10 fT/$\sqrt{\text{Hz}}$, which is high enough to meet research requirements.[8,9] Therefore, it is a promising way to suppress CS noise with a magnetometer.[10–12]

Recently, using OPMs to stabilize magnetic field and suppress noise has been reported. Rosner *et al.* reported a non-magnetic drift optically pumped cesium magnetometer with a measured sensitivity of 35 fT at integration time of 200 s and stability below 50 fT between 70 s and 600 s.[13] Ding *et al.* used an optically pumped potassium magnetometer to suppress the magnetic noise actively and achieved a noise floor of about 100 fT/$\sqrt{\text{Hz}}$ under a bias field from 20 μT to 100 μT.[14] As for the OPM in the study of current noise suppression, Shen *et al.* used an optically pumped Cs atomic magnetometer to suppress the noise of a commercial CS and reached a noise level of 600 pA/$\sqrt{\text{Hz}}$ at 1 Hz.[10] In those studies, the magnetometers they used belonged to double resonance orientation magnetometers (DROMs). However, there is also a class of OPMs called DRAMs (double resonance alignment magnetometers), where the magnetization has the symmetry of an atomic alignment. Compared with DROMs, DRAMs present several potential advantages such as narrow linewidth, insensitivity to light shift, and less affected by the flicker noise of diode lasers.[15–17] We are interested in the ability of DRAMs to perform low-frequency noise suppression, so the main work of this paper is to use DRAMs to suppress current noise below 1 Hz.

2. Experimental equipment and settings

Our experiments are based on two DRAMs and one digital multimeter (Agilent 3458A). The bias magnetic field coils of the two DRAMs are connected in series with an Agilent 3458A. When the CS board output current, we use three devices to simultaneously measure the current's noise. On this

†Corresponding author. E-mail: maxborn@nudt.edu.cn
© 2023 Chinese Physical Society and IOP Publishing Ltd

basis, we conduct the following experimental process. First, we calibrate the voltage-to-current conversion ratio of the CS board and test the frequency response of two DRAMs in the range of 0–10 Hz. Then, we use three devices to measure the current noise of the CS board when it is running freely. Finally, the current noise is suppressed by DRAM A and is measured by DRAM B.

2.1. Experimental setup

The overall experimental device is shown in Fig. 1. The two DRAMs we used have similar structures, so we take DRAM A as an example to briefly introduce the specific structure and parameter settings. A three-axis orthogonal coil located in the center of a five-layer cylindrical magnetic shielding provides the magnetic field we need. A spherical vacuum ^{87}Rb cell with a diameter of 20 mm coated with paraffin is placed in the center of the coil. A distributed Bragg reflection (DBR) laser generates a laser beam. The frequency of the laser beam is locked to $F = 1 \rightarrow F' = 2$ in the D_2 line of the ^{87}Rb and its power is 1 mW. The laser beam transmits through a half-wave plate and a linear polarizer, and then it enters the cylinder perpendicularly to align with the direction of the biased magnetic field. After the beam passes through the cell, a polarimeter composed of a half-wave plate, a lens, a Wollaston prism, and a balanced photodetector (BPD) is used to obtain information about the Faraday rotation angle. The polarimetric signal is sent to a multifunctional lock-in amplifier (HF2LI of Zurich Instruments). After demodulating the signal by HF2LI, the Larmor precession frequency ω_L of the ^{87}Rb atom can be obtained. According to the relationship $\omega_L = \gamma B$, the magnetic field B can be obtained, in which γ is the gyromagnetic ratio of the ^{87}Rb atom. In addition, the HF2LI can also provide a radio-frequency field on a coil perpendicular to the bias magnetic field for magnetic resonance excitation and provide a current-control voltage on the CS board to compensate for the current fluctuations. A rubidium atomic clock provides the frequency reference to the HF2LI. A homemade CS board with a trim port provides currents for the bias magnetic fields of the two DRAMs. However, in this experiment, there are also some different settings between the two DRAMs. To reduce the influence of the possible common-mode magnetic field, we make the axes of the bias magnetic field of the two DRAMs perpendicular to each other. As a result, DRAM B needs to adjust the direction of the optical path by utilizing two extra plane mirrors. No heating of the cell is required for this experiment. Under the control of central air conditioning, the temperature at 2 cm from the cell in DRAM is 24.13 ± 0.05 °C within five days. Under these conditions, we obtain a magnetic resonance signal with a linewidth of approximately 4.2 Hz.

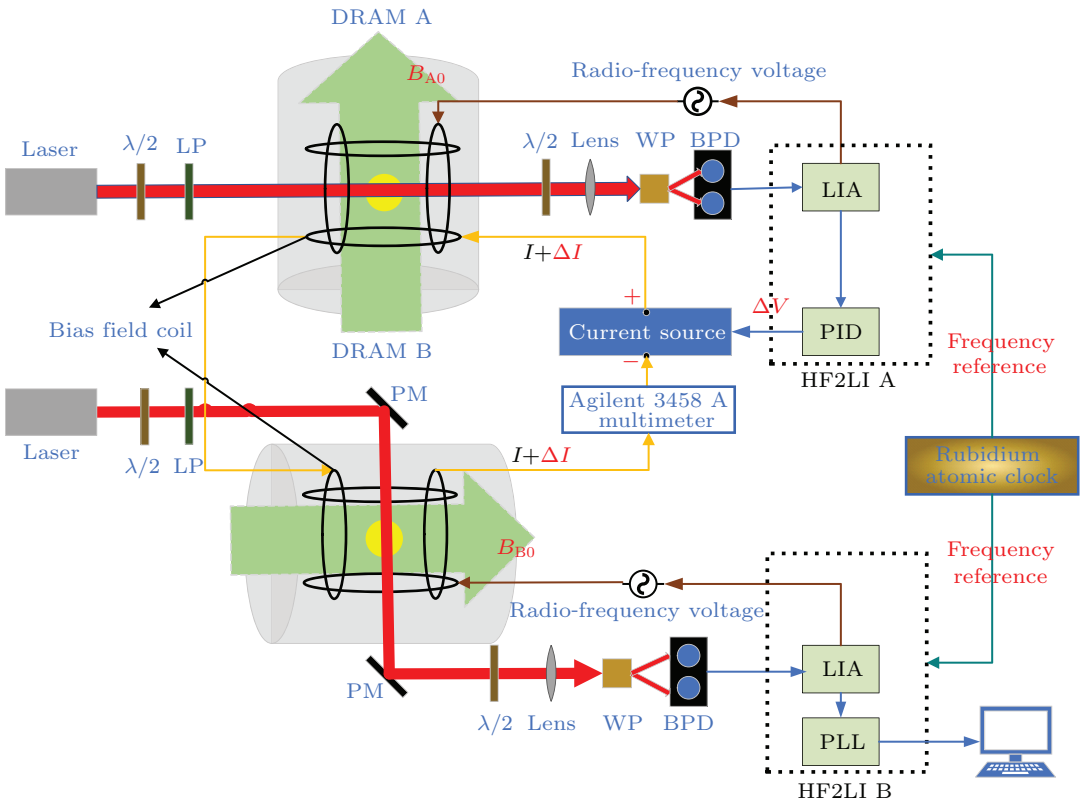


Fig. 1. Experimental setup. LP: linear-polarizer, $\lambda/2$: half-wave plate, lens: convex lens, WP: Wollaston prism, PM: plane mirror, LIA: lock-in amplifier, BPD: balanced photodetector. PID: proportional integral derivative, PLL: phase locked loop. LIA, PID, and PLL are provided by the multi-function lock-in amplifier (HF2LI). B_{A0} and B_{B0} is the bias magnetic fields of the DRAMs, and the bias field directions of the two systems are perpendicular to each other. ΔV is the compensation voltage output by PID. I is the original current source output, ΔI is the compensation current.

3. Results and analysis

Our noise measurement is mainly based on two DRAMs, and the noise suppression process relies on the HF2LI output control voltage to compensate the CS board. A simple compensation implementation diagram is shown in Fig. 2. The current after the first-order steady by the CS board is input into the series loop. DRAM A measures the frequency information ω, and obtains the frequency fluctuation value according to $\omega - \omega_{\text{ref}}$, where ω_{ref} is the reference frequency. The PID (proportional integral derivative) uses the frequency difference to give the compensation voltage, and the compensation voltage is input into the trim port on the CS board to realize the second-order suppression of current noise. DRAM B and Agilent 3458A continuously measure the current in the loop. Therefore, before performing the current noise measurement and suppression, it is necessary to calibrate the coil constants of the two DRAMs, the conversion factor of the CS board to direct current (DC) and alternating current (AC) input voltages, and the frequency response of the two DRAMs. After verifying the reliability of the magnetometer, noise measurement and suppression are performed on our homemade CS board. On this basis, we further discuss how to achieve higher measurement sensitivity and suppression in low-frequency bands.

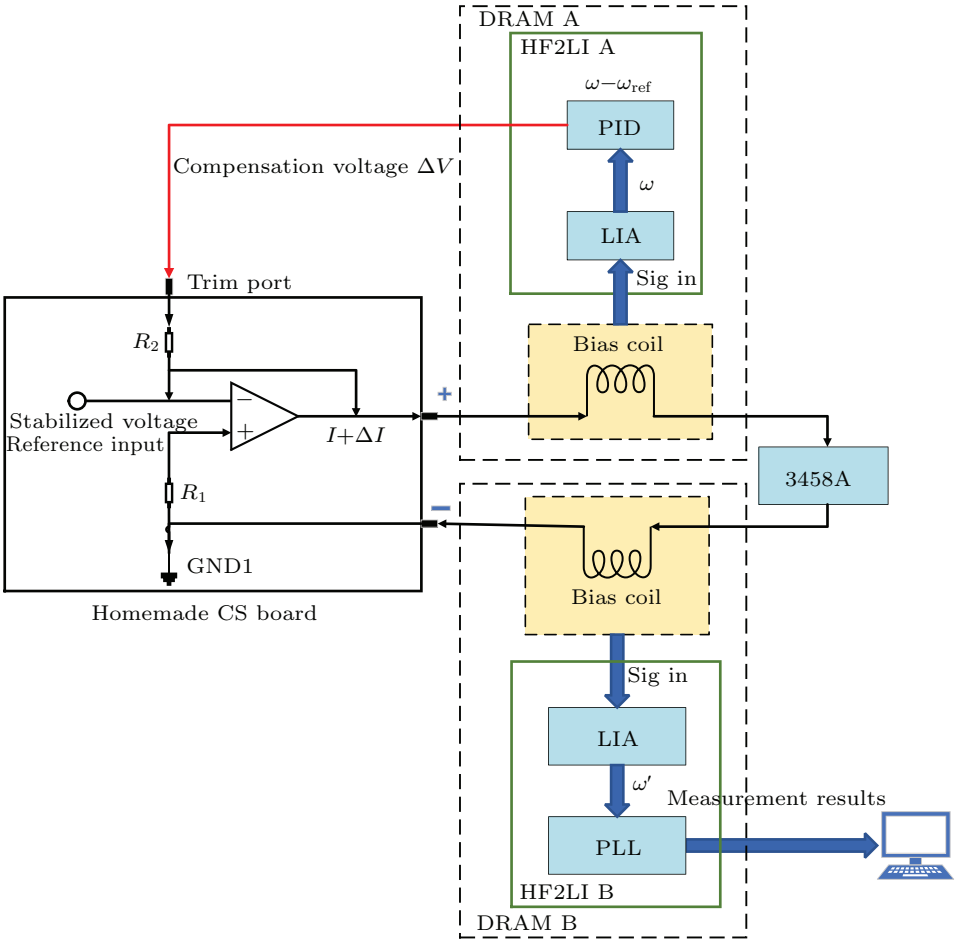


Fig. 2. Compensation implementation diagram. The CS board part only shows how to connect the compensation voltage.

3.1. Parameter calibration

In the experiment, the control voltage produced by the HF2LI is sent to the trim port of the CS board. The output of the CS board connects with an Agilent 3458A digital multimeter and two bias field coils of the two DRAMs in series. Then, by applying a known voltage through the HF2LI, we can use three instruments to measure the current response simultaneously. The measurement results of Agilent 3458A are used as a reference standard for the parameter validation experiments described in the following.

First, we calibrate the coil constants of the bias magnetic fields of the two DRAMs. The two DRAMs measure current based on the formula:

$$I = B/k_{\text{coil}}, \tag{1}$$

where I is current, B is the bias magnetic field, and k_{coil} is coil constant. According to the work of Breschi's E, the coil constants of the bias magnetic field of the two DRAMs are measured, giving $k_{\text{coilA}} = 139.98$ nT/mA and $k_{\text{coilB}} = 107.17$ nT/mA.[18]

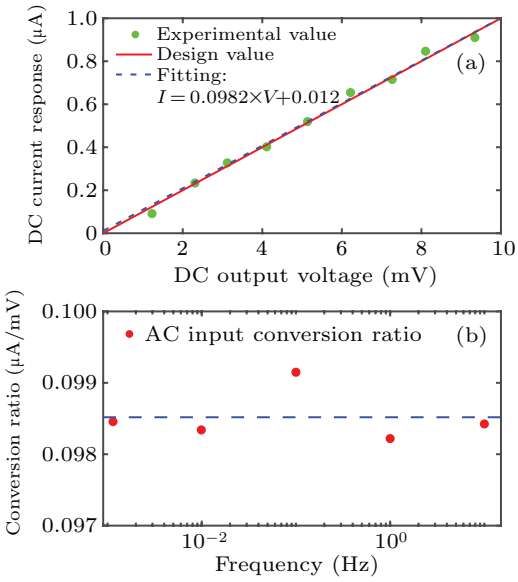


Fig. 3. The conversion factor for DC and AC voltage input. (a) The current response for DC voltage input. The DC voltage–current conversion factor is 0.0982 μA/mV. (b) The conversion factor of the CS board at AC input.

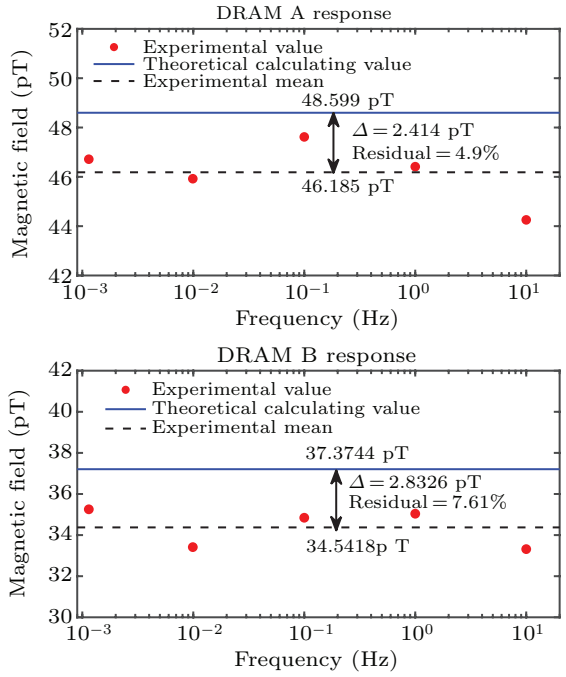


Fig. 4. The response of the DRAMs to AC input. The theoretical response values are 48.599 pT and 37.207 pT, respectively; 46.185 pT and 34.3744 pT are the average values of the experimental data.

Third, we calibrate the frequency response of the magnetometer. Our target frequency band is below 1 Hz. Moreover, because the magnetometer's response is low-pass, we only need to verify that the response is flat within 10 Hz. Considering these factors, we select five frequency points at 0–10 Hz with logarithmic equal spacing. As shown in Fig. 4, by analyzing the power spectrum of the bias magnetic field measured by the DRAMs, we can obtain the frequency responses of DRAMs A and B. In this part, the Agilent 3458A has a 24.25 Hz sampling rate with 0.1 NPLC (number of power line cycles, the larger the NPLC setting, the higher the accuracy and the lower the sampling rate). Moreover, the sampling rates of the HF2LI and the DAQ card are set to 112.4 Hz and 400 Hz, respectively. Among them, the sampling rate of the Agilent 3458A is limited by the sampling program, but it meets our requirements. As for HF2LI and DAQ cards, the settings make a trade-off between performance and data volume. Finally, to obtain sufficient data for power spectrum analysis, we collect the data of 0.001 Hz for 2 h and the data of 0.01 Hz for 1 h. The data of other frequencies are collected for 30 min. According to the measured conversion factors of the CS board and the calibrated coil constant, the theoretical response values of two DRAMs to an AC voltage with 5 mV amplitude are calculated to be 48.599 pT and 37.207 pT. In comparison, the measured responses are correspondingly 46.185 pT and 34.3744 pT. The deviation between the measured results and what we expected for both DRAMs is less than 10%. So far, we verify that the response of the DRAMs is flat in the 0–10 Hz frequency band.

3.2. Current noise measurement and suppression

After confirming the instrument's parameters, we measure the free-running current of the CS board by using two DRAMs and one Agilent 3458A simultaneously. The current of the CS board is 83.438 mA when the voltage applied to the compensation port is removed. Since we are mainly interested in the low-frequency performance, we collect the current for a length of 24 h. The data is analyzed by linear spectral density (LSD), which is defined as the square root of the power spectral density (LSD $= \sqrt{\text{PSD}}$).[19] The results of the three sets of data are shown in Fig. 5. From the LSD analysis results, the noise level measured by the Agilent 3458A in the frequency band above 0.01 Hz is about 450 nA/$\sqrt{\text{Hz}}$. According to the user manual, when NPLC is set as 0.1, the rms noise of the Agilent 3458A is about 1.5 μA, which is divided by the root bandwidth gives about 470 nA/$\sqrt{\text{Hz}}$. Therefore, we know that the LSD given by Agilent 3458A is actually the noise floor of the instrument itself. However, the LSD from both DRAMs shows lower noise levels in this range. Thus, we believe that the results of the DRAM measurements are accurate for several reasons given in the following.

The magnetic field measured by a DRAM can be considered to be derived from B_0 provided by the coil energization and the remaining magnetic field B_r caused by various reasons. The residual magnetic field mainly comes from the influence of the external geomagnetism through the magnetic shield and shield-generated magnetic field from both thermal magnetization noise and Johnson noise currents. At very low frequencies, the noise is dominated by thermal magnetization noise. According to Kornack's work, the magnetic field noise due to magnetization noise in the shield is about 350 fT/$\sqrt{\text{Hz}}$ at 0.0001 Hz.[20] The magnetic shielding material we used is

permalloy, which has high shielding performance against low-frequency noise.[21] The magnetic shielding coefficient of our two systems is about 1×10^6 for DC magnetic fields and AC magnetic fields above 1 Hz. As for the geomagnetic drift of about 200 nT/day, while the shielding coefficient for low frequencies will decrease, it is still in the order of 10^4.[22] After shielding, the fluctuation in the cylinder is estimated to be less than 20 pT/day, which is consistent with Gemmel's work.[23] The noise introduced in the corresponding frequency band is much smaller than the noise level we measured. In addition, the bias field coils of the two DRAMs are orthogonal to each other, so the influence of the common-mode magnetic field is enormously eliminated. The residual magnetic fields in the two DRAMs can be considered irrelevant. Moreover, the coil constants are different, but the LSD of the current is quite coincident. Therefore, we believe that the DRAM's measurement indeed reflects the current noise, and DRAMs have higher resolutions in this set of settings. In addition, there are two possible causes for the 0.8 Hz spike, one is noise shocks introduced by certain frequencies in the device and external environmental changes (e.g., platform vibration), and the other is the phase margin of the internal feedback circuit of the CS board under inductive load (coils A and B).[10] According to LSD shown in Fig. 5, when the CS board is running freely, the noise floor at 0.001 Hz is 1 $\mu A/\sqrt{Hz}$.

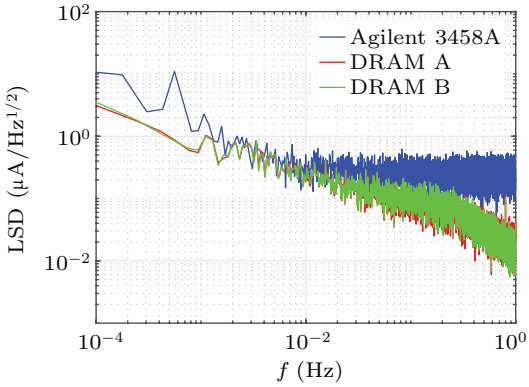


Fig. 5. LSD of Agilent 3458A multimeter and two DRAMs with CS board free running.

Then, we use DRAM A to stabilize the current while using DRAM B and Agilent 3458A as the measurement device. Similarly, we also record data for a length of 24 h. Since the Agilent 3458A cannot reflect the actual noise level of the system when the NPLC parameter is set to 0.1, we change the NPLC to 23, which leads to the sampling rate dropping to 0.8 Hz while the precision increases to 7.5 digits. The closed-loop and open-loop results measured by DRAM B and 3458A are shown in Fig. 6. In addition, using the Agilent 3458A with the setting, we re-measure the current noise when the CS board is free running. This set of results is also plotted in Fig. 6. First of all, it is evident that when the Agilent 3458A improves its accuracy, it can reflect the noise level of the CS board without compensation, and the results of the 3458A measurements are in good agreement with the DRAM, which is an excellent testament to conclude that the noise introduced by the residual magnetic field is a small amount. However, with the compensation of the CS board, the Agilent 3458A loses the ability to reflect the actual current noise level when the CS noise is further reduced. Also, the noise introduced by the residual magnetic field is still much smaller than the measured result after compensation. Therefore, we believe that the measurement results for DRAM B are credible, and the measurement is current noise. When the CS board takes compensation, the noise drift is suppressed by about 10 times in the frequency range of 0.001–0.1 Hz, and it is also suppressed by about 5 times at 1 Hz. The current noise level at 0.001 Hz is lower than 100 $nA/\sqrt{Hz}$. As for the noise drifting quickly below 0.001 Hz, we believe that it is caused by the drift of the magnetometer. How to reduce the noise drift of lower frequencies awaits further research after system upgrades in the future.

The above open-loop and closed-loop current values recorded by DRAM B are analyzed by using the Allan equation. The relative Allan deviations are shown in Fig. 7. It is evident that when the CS board is compensated, the stability of the CS board is improved from 5×10^{-7} to 2.2×10^{-8}, and the stability is below 10^{-7} between 20 s and 3000 s.

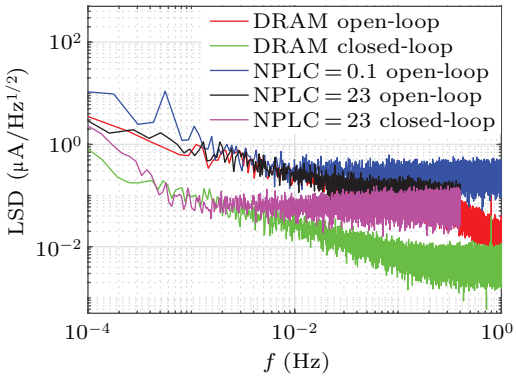


Fig. 6. LSD comparison between the Agilent 3458A for two sets of NPLC parameters and DRAM B for open-loop and closed-loop. Because there are only 0.8 Hz samples for Agilent 3458A at NPLC = 23, the results of the Agilent 3458A only show a frequency band below 0.4 Hz.

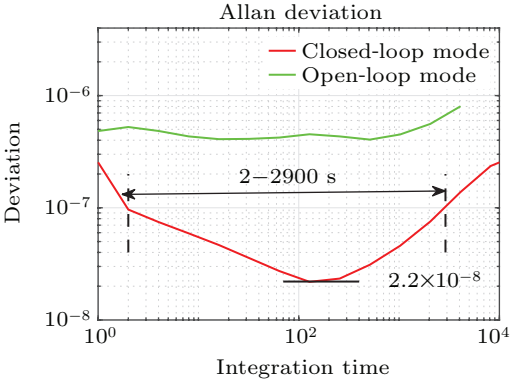


Fig. 7. The relative Allan variance comparison of a set of open-loop current and a set of closed-loop current.

3.3. Optimization discussion

We seek to obtain a more stable magnetometer state on the existing adjustable experimental parameters. We tune the laser frequency of DRAMs A and B to far away from the resonant state about 1.1 GHz. Under this condition, the magnetic resonance linewidth becomes larger and the signal-to-noise ratio decreases. Likewise, we use DRAM A to compensate the board and DRAM B for measuring the current. The LSD of the measured current before and after laser frequency tuning is shown in Fig. 8.

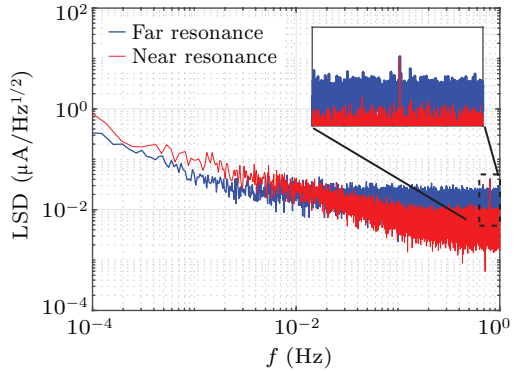


Fig. 8. The LSD comparison between near-resonance and far-resonance DRAM B laser frequencies.

Below 0.01 Hz, DRAMs at far resonant laser frequencies have lower drift because the interaction between the light and atoms becomes weaker when the laser is far from resonance, and the variation of laser parameters has a smaller influence on the drift of DRAM. As for the frequency band higher than 0.01 Hz, due to the far-resonance conditions providing a lower signal-to-noise ratio, the far resonance noise level is higher than the near resonance noise level. To demonstrate this explanation, we tune the frequency from the resonant state to the far-resonant state with a 100 MHz step length. The resonance linewidth and amplitude under different detuning amounts are shown in Fig. 9. Meanwhile, according to Zhivun's work, the data is fitted. His work shows that the broadening is induced by the real transitions, it is proportional to the absorption probability $1/(f^2+f_0^2)$, where f_0 is the resonant position laser frequency and f is the actual laser frequency.[24] With the increasing detuning, the resonance linewidth gradually becomes smaller, and the resonance amplitude also becomes smaller. Among them, the linewidth in the near-resonance region varies more significantly with the amplifying detuning, and the resonance linewidth in the far-resonance region varies relatively gently with the increase in detuning. This phenomenon is an excellent illustration to explain why detuning the laser frequency can reduce low-frequency noise. The results shown in Fig. 8 also prove that the sensitivity of the magnetometer limits the DRAM's suppression current of low-frequency noise.

Based on the experience of the experimental process and the analysis of the final results, we expect that the suppression of low-frequency noise can still be improved in the following aspects.

First, reducing the environment temperature's influence on the device can directly improve the current noise suppression level.[25] For example, a temperature compensation mechanism can be designed for the standard resistance in the CS board, a magnetic shielding material with a smaller temperature coefficient can be used, and the temperature control system of the laser can be upgraded. These methods can attenuate the low-frequency drift caused by ambient laboratory temperature fluctuations.[26]

Second, using a DRAM with higher sensitivity and stability at low frequencies to build closed-loop control is likely to suppress the CS noise further. For example, under the condition of not producing a large magnetic field gradient, the coil constant can be optimized as large as possible.[27–29] The laser frequency can be adjusted, and the cell can be heated properly and stably. In addition, eliminating the magnetic field gradient and optimizing the laser parameters can also give the DRAM higher sensitivity to achieve the higher resolution magnetometer we expected.[30]

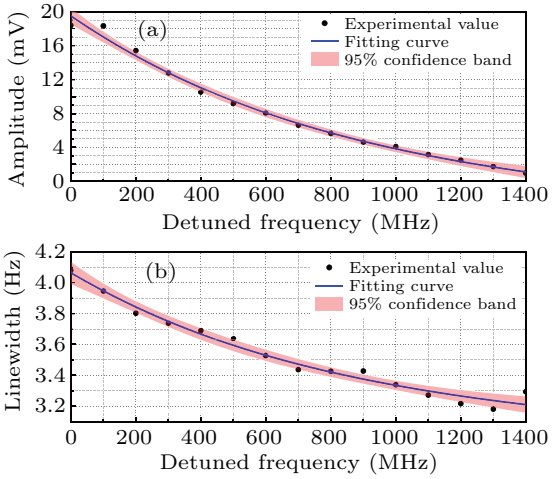


Fig. 9. The resonance linewidth and amplitude under different detunings of laser frequencies.

4. Conclusion and perspectives

We measure and suppress current noise in the low-frequency region by using DRAMs. The significance of this work is summarized in the following three aspects: (i) The noise suppression using DRAM achieves excellent performance at 0.0001–1 Hz. If the stability is evaluated by LSD, the CS board noise level can be suppressed to 100 $\mathrm{nA}/\sqrt{\mathrm{Hz}}$ at 0.001 Hz. (ii) By designing the CS board and using DRAM to form a closed-loop compensation, we obtain a CS board with the stability of 2.2×10^{-8}, which is an excellent reference for building a CS board with low noise and high stability in fundamental physics research. (iii) Compared with the Aglient 3458A multimeter, using DRAMs to evaluate CS has the advantages of higher resolution and broader response bandwidth.

Under our experimental conditions, DRAMs are more accurate for current measurements.

Finally, the performance of the DRAMs can be further improved by optimizing their parameters. Moreover, combination of DRAMs with DROMs may achieve high-precision current measurement and noise suppression ability in the range of 0.001–1000 Hz, which is an attractive commercial development scheme for CS.

Acknowledgements

We want to thank the team of Professor Hong Guo at Peking University and Professor Xiang Peng for providing a narrow linewidth atomic cell. At the same time, I would like to thank Tianyu Qian for his help in writing.

Project supported by the National Natural Science Foundation of China (Grant Nos. 12174446 and 61671458).

References

[1] Kitching J, Donley E A, Knappe S, Hummon M, Dellis A T, Sherman J, Srinivasan K, Aksyuk V A, Li Q, Westly D, Roxworthy B and Lal A 2016 *J. Phys.: Conf. Ser.* **723** 012056

[2] Afach S, Budker D, DeCamp G, *et al.* 2018 *Phys. Dark Universe* **22** 162

[3] Chupp T E, Fierlinger P, Ramsey-Musolf M J and Singh J T 2019 *Rev. Mod. Phys.* **91** 015001

[4] Wurm D, Beck D H, Chupp T *et al.* 2019 *EPJ Web Conf.* **219** 02006

[5] Allmendinger F, Heil W, Karpuk S, Kilian W, Scharth A, Schmidt U, Schnabel A, Sobolev Yu and Tullney K 2014 *Phys. Rev. Lett.* **112** 110801

[6] Terrano W A and Romalis M V 2021 *Quantum Sci. Technol.* **7** 014001

[7] Furukawa T, Inoue T, Nanao T, Yoshimi A, Tsuchiya M, Hayashi H, Uchida M and Asahi K 2011 *J. Phys.: Conf. Ser.* **312** 102005

[8] Castagna N, Bison G, Di Domenico G, Hofer A, Knowles P, Macchione C, Saudan H and Weis A 2009 *Appl. Phys. B* **96** 763

[9] Taylor J M, Cappellaro P, Childress L, Jiang L, Budker D, Hemmer P R, Yacoby A, Walsworth R and Lukin M D 2008 *Nat. Phys.* **4** 810

[10] Shen L, Zhang R, Wu T, Peng X, Yu S, Chen J and Guo H 2020 *Rev. Sci. Instrum.* **91** 084701

[11] Rosner M, Beck D, Fierlinger P, Filter H, Klau C, Kuchler F, Rößner P, Sturm M, Wurm D and Sun Z 2022 *Appl. Phys. Lett.* **120** 161102

[12] Chen D Y, Miao P X, Shi Y C, Cui J Z, Liu Z D, Chen J and Wang K 2022 *Acta Phys. Sin.* **71** 024202 (in Chinee)

[13] Rosner M, Beck D, Fierlinger P, Filter H, Klau C, Kuchler F, Rößner P, Sturm M, Wurm D and Sun Z 2022 *Appl. Phys. Lett.* **120** 161102

[14] Ding Y, Zhang R, Zheng J, Chen J, Peng X, Wu T and Guo H 2022 *Rev. Sci. Instrum.* **93** 015003

[15] Weis A, Bison G and Pazgalev A S 2006 *Phys. Rev. A* **74** 033401

[16] Mathur B S, Tang H and Happer W 1968 *Phys. Rev.* **171** 11

[17] Di Domenico G, Bison G, Groeger S, Knowles P, Pazgalev A S, Rebetez M, Saudan H and Weis A 2006 *Phys. Rev. A* **74** 063415

[18] Breschi E, Grujić Z and Weis A 2014 *Appl. Phys. B* **115** 85

[19] Heinzel G, Rüdiger A and Schilling R 2002 http://hdl.handle.net/11858/00-001M-0000-0013-557A-5 [2002]

[20] Kornack T W, Smullin S J, Lee S K and Romalis M V 2007 *Appl. Phys. Lett.* **90** 223501

[21] Keshtkar A, Maghoul A and Kalantarnia A 2011 *Int. J. Comput. Electr. Eng.* **3** 507

[22] Altarev I, Bales M, Beck D H, *et al.* 2015 *J. Appl. Phys.* **117** 183903

[23] Gemmel C, Heil W, Karpuk S, Lenz K, Ludwig Ch, Sobolev Yu, Tullney K, Burghoff M, Kilian W, Knappe-Grüneberg S, Müller W, Schnabel A, Seifert F, Trahms L and Baeßler St 2010 *Eur. Phys. J. D* **57** 303

[24] Zhivun E 2016 *Ph.D. Dissertation* (Berkeley: University of California, Berkeley)

[25] Fan W, Liu G, Li R, Quan W, Jiang L and Duan L 2017 *Meas. Sci. Technol.* **28** 095007

[26] Stoller S D, Happer W and Dyson F J 1991 *Phys. Rev. A* **44** 7459

[27] Golub R, Rohm R M and Swank C M 2011 *Phys. Rev. A* **83** 023402

[28] Fu Y Y and Yuan J 2017 *AIP Adv.* **7** 115315

[29] Zheng W, Gao H, Liu J G, Zhang Y, Ye Q and Swank C 2011 *Phys. Rev. A* **84** 053411

[30] Yang K, Lu J, Ma Y, Wang Z, Sun B, Wang Y and Han B 2022 *IEEE Trans. Instrum. Meas.* **71** 1501108